Decellularized extracellular matrix particle-based biomaterials for cartilage repair applications

Author(s):
Guo, Peng; Jiang, Nan; Mini, Carina; Miklosic, Gregor; Zhu, Songsong; Vernengo, Andrea J.; D'Este, Matteo; Grad, Sibylle; Alini, Mauro; Li, Zhen

Publication date:
2023-10-10

Permanent link:
https://doi.org/10.3929/ethz-b-000614589

Originally published in:
Journal of Materials Science and Technology 160, https://doi.org/10.1016/j.jmst.2023.03.019

Funding acknowledgement:
189310 - INDEED - Engineered full-organ 3D intervertebral disc as standardized model for studying disc degeneration and disease (SNF)

Journal of Materials Science & Technology 160 (2023) 194–203

Contents lists available at ScienceDirect

Journal of Materials Science & Technology

journal homepage: www.elsevier.com/locate/jmst

Research Article

Decellularized extracellular matrix particle-based biomaterials for cartilage repair applications

Peng Guo[a,b], Nan Jiang[a,c], Carina Mini[a], Gregor Miklosic[a,d], Songsong Zhu[c], Andrea J. Vernengo[a], Matteo D'Este[a], Sibylle Grad[a], Mauro Alini[a], Zhen Li[a,*]

[a] AO Research Institute Davos, Davos 7270, Switzerland
[b] Department of Spine Surgery, The Sixth Affiliated Hospital, Sun Yat-sen University, Guangzhou 510655, China
[c] State Key Laboratory of Oral Diseases and National Clinical Research Center for Oral Disease and West China Hospital of Stomatology, Sichuan University, Chengdu 610041, China
[d] Institute for Biomechanics, ETH Zürich, Zürich 8093, Switzerland

ARTICLE INFO

Article history:
Received 16 May 2022
Revised 20 February 2023
Accepted 2 March 2023
Available online 19 April 2023

Keywords:
Cartilage tissue engineering
Decellularized extracellular matrix
Proteoglycan integrity
Biomimetic hydrogels
Biomaterial
Bioink

ABSTRACT

Cartilage Decellularized ExtraCellular Matrix (dECM) materials have shown promising cartilage regeneration capacity due to their chondrogenic bioactivity. However, the limited retention of ECM components and the reduced integrity of functional ECM molecules during traditional decellularization processes impair the biomimicry of these materials. The current study aims to fabricate biomimetic materials containing decellularized cartilage particles that have an intact molecular structure and native composition as biomaterial inks and hydrogels for cartilage repair. For this, we established a novel two-fraction decellularization strategy for the preparation of reconstituted dECM (rdECM) particles by mixing the two-fraction components, as well as a one-fraction decellularization strategy for the preparation of biomimetic dECM (bdECM) particles. Hyaluronic acid-tyramine (THA) hydrogels containing rdECM or bdECM particles were produced and characterized via rheological test, swelling and stability evaluation, and compression test. The results showed that our novel decellularization strategies preserved intact proteoglycans and collagen at a higher retention rate with adequate DNA removal compared to traditional methods of decellularization. The addition of rdECM or bdECM particles significantly increased the shear moduli of the THA bioinks while preserving their shear-thinning properties. bdECM particle-embedded THA hydrogels also achieved long-term stability with a swelling ratio of 70% and high retention of glycosaminoglycans and collagen after long-term incubation, while rdECM particle-embedded THA hydrogels showed unsatisfactory stability as self-standing biomaterials. Compared to pure THA hydrogels, the addition of bdECM particles significantly enhanced the compression moduli. In summary, our decellularization methods are successful in the retention of functional and intact cartilage components with high yield. Both rdECM and bdECM particles can be supplemented in THA bioinks for biomimetic cartilage 3D printing. Hydrogels with cartilage bdECM particles possess the functional structure and the natural composition of cartilage ECM, long-term stability, and enhanced mechanical properties, and are promising biomaterials for cartilage repair.

1. Introduction

Due to the low cell density, avascularity, and lack of innervation, cartilage has a poor capacity for self-healing [1]. Currently, there is no effective treatment for degenerative or traumatic cartilage defects. Cartilage tissue engineering is a promising method to address these problems [2]. Due to its resemblance to the natural microenvironment and chondrogenic bioactivity, cartilage ExtraCellular Matrix (ECM) shows a beneficial effect on tissue morphogenesis, differentiation, and homeostasis. ECM biomaterials have promising regeneration capacity for cartilage tissue engineering [3,4].

Successful decellularization of cartilage tissue to remove its native cells and genetic material is required to eliminate the immunogenicity of decellularized ECM (dECM) for tissue engineering applications. Although many cartilage decellularization

* Corresponding author.
E-mail address: zhen.li@aofoundation.org (Z. Li).

https://doi.org/10.1016/j.jmst.2023.03.019

methods have been published [5,6], there is still a lack of consensus on superior methods. The common decellularization methods for articular cartilage involve a combination of chemical (e.g. acids/alkalines, chelating agents, ionic/non-ionic/zwitterionic detergents), enzymatic (e.g. proteases, nucleases), and physical (e.g. mechanical agitation, freeze/thaw cycles, hydrostatic pressure, osmotic pressure, perfusion, supercritical CO_2, sonication) processes [7]. Due to the dense nature of the cartilage ECM, which creates an obstacle to the diffusion of reagents, decellularization protocols often include harsh steps involving high amounts of various proteases and detergents to achieve enhanced tissue permeabilization. This leads to a significant loss of sulfated glycosaminoglycans (GAG), collagen, and growth factors, as well as disruption of proteoglycan (PG) integrity that is ignored in most previous studies [3,8,9]. Improvements in cartilage decellularization methods are needed to effectively remove cellular and genetic components while preserving the cartilage ECM composition and ultrastructural integrity of functional ECM components.

In addition, except for acting as standalone biomaterials, dECM is usually manufactured as solubilized components to obtain a homogeneous regenerative microenvironment for tissue engineering [10]. However, dECM components, especially collagens, have very limited solubility, which is far from the physiological concentration in cartilage tissue [11]. The solubilization process of dECM components also significantly damages the integrity of functional molecules [12], which impairs their biomimicry for cartilage regeneration. To avoid these issues, dECM components can be prepared as particles to retain their structural integrity for the fabrication of biomaterials [9,13]. Compared to solubilized dECM, particle-based dECM components can also improve the porosity and mechanical properties of biomaterials [9]. However, particles alone can hardly sustain the 3D architecture of biomaterials without a supporting system to keep them in position. With the advantages of biomimetic molecular structure and composition, and control over their shapes, hydrogels containing dECM particles may be a promising strategy for cartilage regeneration. However, it is still challenging to restore both intact structure and natural composition of cartilage components in dECM particle-based hydrogels.

In this study, we established two novel protease-/detergent-free cartilage decellularization strategies. The two-fraction strategy generates two separate dECM components which can be mixed to fabricate reconstituted dECM (rdECM) particles. The one-fraction strategy generates intact biomimetic dECM (bdECM) particles to achieve the biomimetic ECM structure, composition and function. Decellularization efficiency and the retention and integrity of functional ECM components were characterized. Since hyaluronic acid (HA) is a natural component of cartilage ECM, an HA hydrogel system containing dECM components would contribute to the restoration of the natural biomimetic composition of cartilage. Therefore, we selected hyaluronic acid-tyramine (THA) for fabricating rdECM or bdECM composite hydrogels with intact molecular structure and native composition of collagen and PG. We evaluated the printability of particle-embedded THA hydrogels as biomaterial inks, as well as their mechanical properties, swelling behavior, and stability for usage as biomaterials for cartilage healing or repair.

2. Materials and methods

2.1. Cartilage collection

The cartilage for this study was collected from bovine knee joints (16 animals, 276–380 days old) within 48 h of slaughter. Cartilage tissue was harvested by exposure of the knee joint cavity and collection of full-thickness cartilage slices using scalpels, with care not to include any calcified tissue. Harvested tissue fragments were washed with phosphate-buffered saline (PBS, Sigma Aldrich, USA) and immediately frozen at −20 °C until further processing.

2.2. Decellularization

Cartilage tissue fragments were treated with five cycles of freeze/thaw (−20 °C, 16 h/room temperature, 8 h) followed by pulverization in a liquid nitrogen Mixer Mill (MM 400, Retsch) at 25 Hz for 3 min. The pulverized tissue pieces showed a relatively consistent size of 339 ± 186 μm. Pulverized tissue was exposed to one of four treatments at 4 °C with agitation for 24 h: (1) 5% (*w*/*v*) sodium dodecyl sulfate (SDS, Sigma Aldrich, USA) pretreatment [14], (2) 1% (*v*/*v*) Triton X-100 (Sigma Aldrich, USA) pretreatment [15], (3) milli-Q water pretreatment, (4) no pretreatment. The SDS and Triton X-100 groups represent decellularization methods using invasive detergents. Pretreated cartilage tissue underwent 6 rinses in milli-Q water with a total rinse time of 6 h to thoroughly remove the detergent reagents [7,9,16,17]. After pretreatment and rinsing, DNase I (100 U/mL, Sigma Aldrich, USA) with protease inhibitor cocktail (0.2% v/v, Sigma Aldrich, USA) treatment for 8 h was applied to remove cellular DNA. One/two-fraction dECM production procedures were then processed as described below (Fig. 1):

(1) Two-fraction production strategy: To mimic the different physiochemical properties of native cartilage tissue from various cartilage layers or anatomic locations, the reconstitution of separate ECM components would contribute to the precise control of the biomimetic composition of the dECM biomaterials. In the two-fraction strategy, the PGs and water-soluble proteins were separated from the insoluble components (mainly collagens) using previously established guanidine-hydrochloric acid (GuHCl)-based procedures [18]. Briefly, decellularized tissue was soaked in GuHCl extraction buffer (4 M GuHCl (Fluka, USA), 50 mM sodium acetate (Sigma Aldrich, USA), pH 5.8, 10 mM EDTA (Sigma Aldrich, USA) with 0.2% (v/v) protease inhibitor cocktail) at 4 °C with shaking for 48 h as previously described [19]. The supernatant was further dialyzed with a 12–14 kDa dialysis membrane (SpectraPor®, USA) at 4 °C for a total duration of 2 days. After dialysis, the sample was collected for lyophilization to generate soluble (SOL) extract. Meanwhile, the remaining cartilage tissue after GuHCl extraction was lyophilized to produce remaining insoluble (INSOL) tissue.

(2) One-fraction production strategy: In addition to the biomimetic composition of dECM biomaterials, the one-fraction strategy retains the natural interaction and connection of functional components without the separation of PG and collagen in cartilage tissue. After the above-described procedures of freeze/thaw cycles, pulverization, pretreatment, and DNase digestion, decellularized tissue was directly lyophilized to generate bdECM tissue.

2.3. Preparation of cartilage acellular ECM particles

INSOL and bdECM tissues were used to prepare INSOL and bdECM particles respectively through a re-homogenization procedure via pulverization in a liquid nitrogen Mixer Mill at 25 Hz for 15 min. The particle size was visualized under a microscope (Olympus BX63, Japan) and quantified using ImageJ 1.53c (National Institutes of Health, USA).

2.4. Characterization of the decellularized components

2.4.1. Biochemical analysis

Lyophilized fresh cartilage, bdECM/INSOL particles, and SOL extract were analyzed for biochemical quantification. Samples (10 mg) were digested in 1 mL of Proteinase K (1 mg/mL, Roche, Switzerland) at 56 °C overnight. DNA quantification was carried

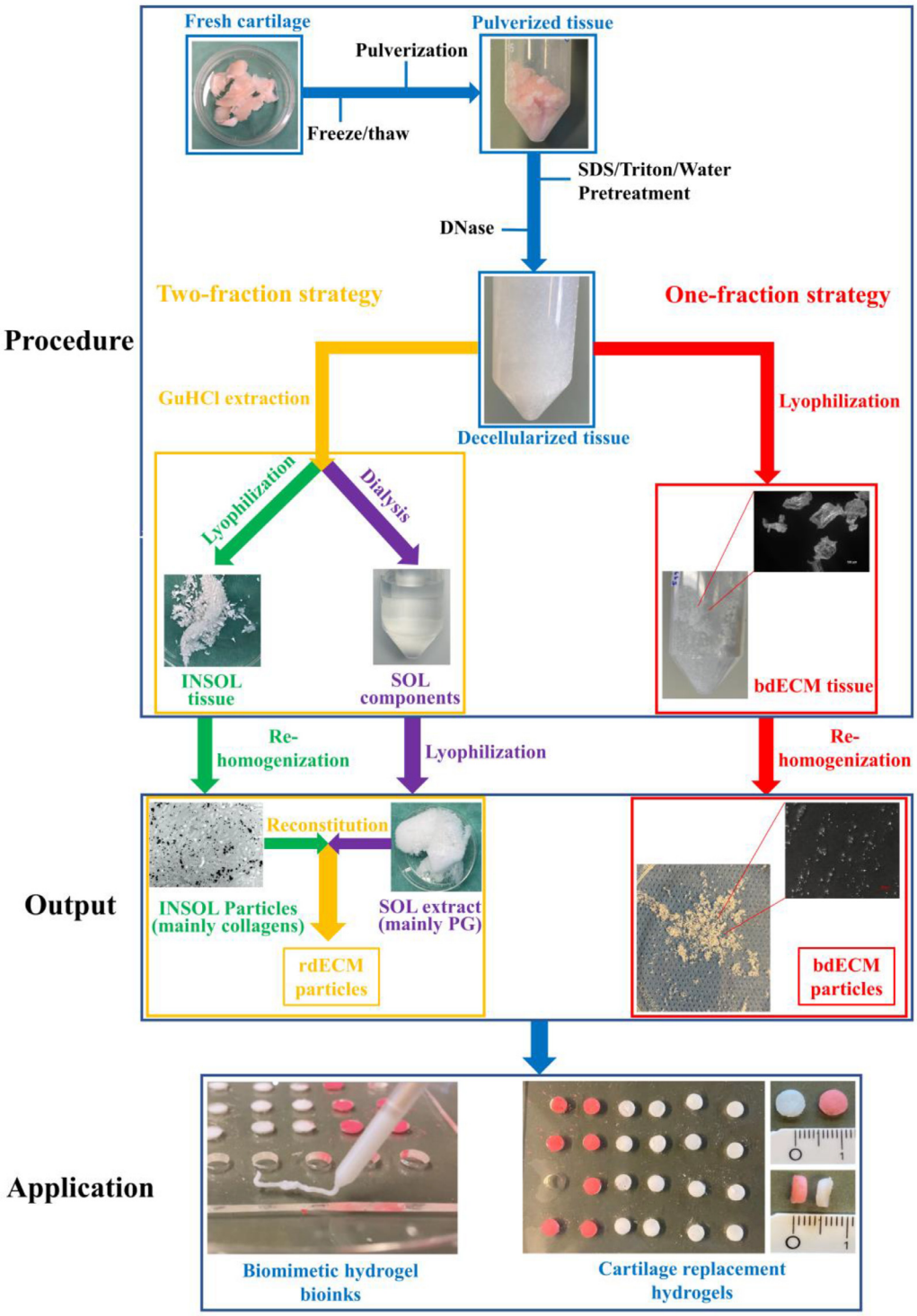

Fig. 1. Schematic illustration of the production of decellularized extracellular matrix particle-based hydrogels as biomaterials for cartilage repair applications.

out using the PicoGreen assay (Thermo Fisher, USA) according to the manufacturer's protocol. GAG concentration was quantified using the 1,9-dimethylmethylene blue (DMMB, Sigma Aldrich) assay at a wavelength of 535 nm. Collagen concentration was measured with hydroxyproline assay after NaOH hydrolysis (Sigma Aldrich, USA) and neutralization with citric acid (Sigma Aldrich, USA).

2.4.2. Agarose gel electrophoresis

Proteins and proteoglycans were extracted with GuHCl-based solutions and precipitated with 100% ethanol. Agarose gel electrophoresis was used for the evaluation of proteoglycan integrity as previously described [20,21]. The gels were imaged with a Chemi Genius Bio-Imaging system (Syngene, USA).

2.4.3. Safranin O/Fast green staining

Fresh cartilage tissue specimens and INSOL/bdECM tissue were embedded in the tissue freezing medium (Leica, Germany) for snap-freezing. Snap-frozen samples were sectioned into 10 μm frozen sections with a cryostat microtome (Leica, Germany) for histological staining. After fixation with 70% methanol and 100%

methanol in sequence, slides were stained with 0.1% Safranin O (Sigma Aldrich, USA) and 0.02% Fast Green (Sigma Aldrich, USA) in 0.1% acetic acid to visualize PG and collagen distribution. Weigert's hematoxylin (Merck, USA) counterstain was performed to visualize the cell nucleus [22].

2.5. Preparation of particle-embedded THA hydrogels

THA was synthesized by grafting tyramine to the carboxyl groups of hyaluronic acid via amide bond formation in water as previously described [23–27]. The degree of substitution was 6.2% as determined by absorbance reading at 275 nm using tyramine hydrochloride as a standard. rdECM particles were prepared by mixing the SOL extract and INSOL particles into the THA solution.

(1) THA hydrogel bioinks: THA (1%, 3% *w*/*v*) and bdECM or rdECM particles (20% w/w) were reconstituted with PBS containing 0.1 U/mL horseradish peroxidase (HRP; Sigma Aldrich, USA) at 4 °C under agitation for 24 h. Enzymatic crosslinking was initiated by adding 5 ppm hydrogen peroxide (H_2O_2, Sigma Aldrich, USA) and incubation for 30 min at 37 °C.

(2) THA biomimetic hydrogels: THA and bdECM or rdECM particles were reconstituted with PBS containing 0.1 U/mL HRP. Enzymatic cross-linking was initiated by adding 5 ppm H_2O_2 in custom-made molds and incubating for 30 min at 37 °C. Additional light crosslinking was performed via exposure to green light (518 nm) for 30 min at 37 °C with 0.2 mg/mL of eosin Y (Sigma Aldrich, USA) as the photoinitiator.

2.6. Evaluation of THA hydrogels

2.6.1. Rheological characterization

Rheological measurements were performed on an Anton PaarMCR 302 rheometer with parallel plate geometry ($d = 25$ mm) and a Peltier temperature control device with a thermostatic hood ($T = 37.00 \pm 0.02$ °C). The gap was set at 300 µm, and a layer of low-viscosity silicon oil was distributed along the sample edge to prevent evaporation. Gelation time ($t = 1800$s, $\gamma = 0.1\%$, $f = 1$ Hz), strain-dependent response ($\gamma = 0.1$–1000%, $f = 1$ Hz) and elastic recovery were evaluated in oscillation. Viscosity was determined rotationally for shear rates from 0.1 to 100 s^{-1}.

2.6.2. Swelling and stability evaluation

Sterile hydrogels (cylinder, 5 mm in diameter and 3 mm in height) were pre-weighed (W_p), and then incubated in Dulbecco's Modified Eagle Medium (DMEM, Gibco) within a 37 °C humidified incubator. The medium was removed at different time points, followed by another weighing (W_w). The swelling ratio was calculated using the equation:

$$\text{Swelling ratio } (\%) = \frac{W_w - W_p}{W_p} \times 100 \quad (1)$$

The release of GAG and collagen into the medium was determined by soaking particle-embedded hydrogels in DMEM. The initial content of GAG and collagen (W_e) was calculated based on the weight of the gel and the particle concentrations added during preparation. Culture medium was collected at specified time points and hydrogels were transferred into fresh DMEM. Released GAG and collagen in the culture medium were then quantified by DMMB and hydroxyproline assays ($W1$, $W2$, $W3$…). GAG and collagen retention and cumulative release ratio were calculated using the following equations:

$$\text{Cumulative release ratio } (\%) = \frac{W1 + W2 + W3 + \ldots}{W_e} \times 100 \quad (2)$$

$$\text{Retention } \left(\frac{\mu g}{\text{mg}}\text{gel weight}\right) = W_e - (W1 + W2 + W3 + \ldots) \quad (3)$$

2.6.3. Compression test

Unconfined uniaxial compression tests were conducted on hydrogels containing different concentrations of bdECM particles, using an Instron electromechanical testing machine (Model 5866, High Wycombe, UK) equipped with a 10 N load cell. Fresh bovine cartilage tissue at the same dimension was measured as the positive control. Samples were measured after equilibration in DMEM for 30 min and subjected to a displacement ramp (0.5 mm min^{-1}) until failure. The stress–strain curve was used to calculate the compressive tangent modulus by measuring the slope of the linear region in the range of 10%–20% strain using Matlab (R2018, MathWorks®).

2.7. Statistical analysis

The statistical analyses were performed using SPSS 25.0 software. The Shapiro-Wilk normality test was used to determine whether the data were normally distributed. For data that were normally distributed, unpaired *t*-test was used to compare two groups and one-way ANOVA was used to compare three or more groups. For data that were not normally distributed, Mann-Whitney U test was used to compare two groups, and Kruskal-Wallis test was used to compare three or more groups. $P < 0.05$ was considered statistically significant.

3. Results and discussion

3.1. Characterization of cartilage dECM components produced by the two-fraction strategy

Different cartilage types, such as fibrocartilage and hyaline cartilage, or even different cartilage zones, have different collagen and GAG content [3,28]. Considering the diverse composition of native cartilage tissue, the extraction of functional decellularization components would be helpful and necessary for the preparation of biomimetic biomaterials. Through the reconstitution of separated functional components at controlled composition ratios, customized biomaterials can be precisely manufactured. To extract functional decellularized cartilage components separately with high yield, we established a two-fraction strategy (Fig. 1). Physical treatments are the least disruptive decellularization methods and preserve most of the ECM composition and intact structure [29]. Among these, freeze-thaw decellularization shows clear advantages [30]. However, a combination of additional methods is required since the cellular components cannot be completely removed by physical decellularization alone [31]. Considering the limited diffusion of chemical or enzymatic reagents into the dense cartilage matrices, additional treatment, such as physical pulverization to increase the surface area and enhance the permeation of chemical and enzymatic agents into the tissue, would improve the efficiency of decellularization [3]. To retain the intact ECM components as much as possible, we combined freeze/thaw cycles with pulverization to reduce the harshness of the chemical or enzymatic decellularization as much as possible.

PGs, of which aggrecan is the most prevalent type in cartilage, and collagens, with type I and II collagens being the most abundant, are the main components of cartilage ECM. The two-fraction strategy aimed to extract decellularized PG and collagen separately. Fig. 2 shows the DNA concentration (ng/mg tissue dry weight) in different tissues after decellularization. Pretreatments of SDS and Triton X-100 significantly decreased the DNA content within the cartilage tissue. Our two-fraction strategy alone (no pretreatment group) was also sufficient to achieve adequate nucleic acid

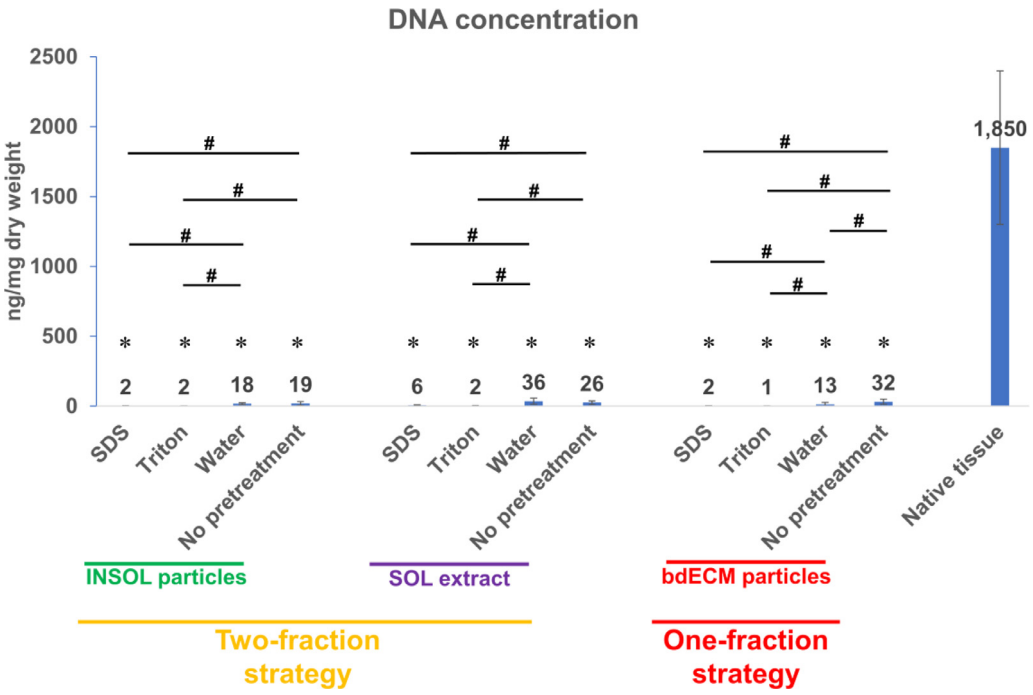

Fig. 2. The DNA concentration in INSOL particles and SOL extract from two-fraction decellularization strategy, and bdECM particles from one-fraction strategy with different pretreatments. Data presented as mean ± SD, $n = 9$, * $p < 0.05$ vs native tissue, # $p < 0.05$.

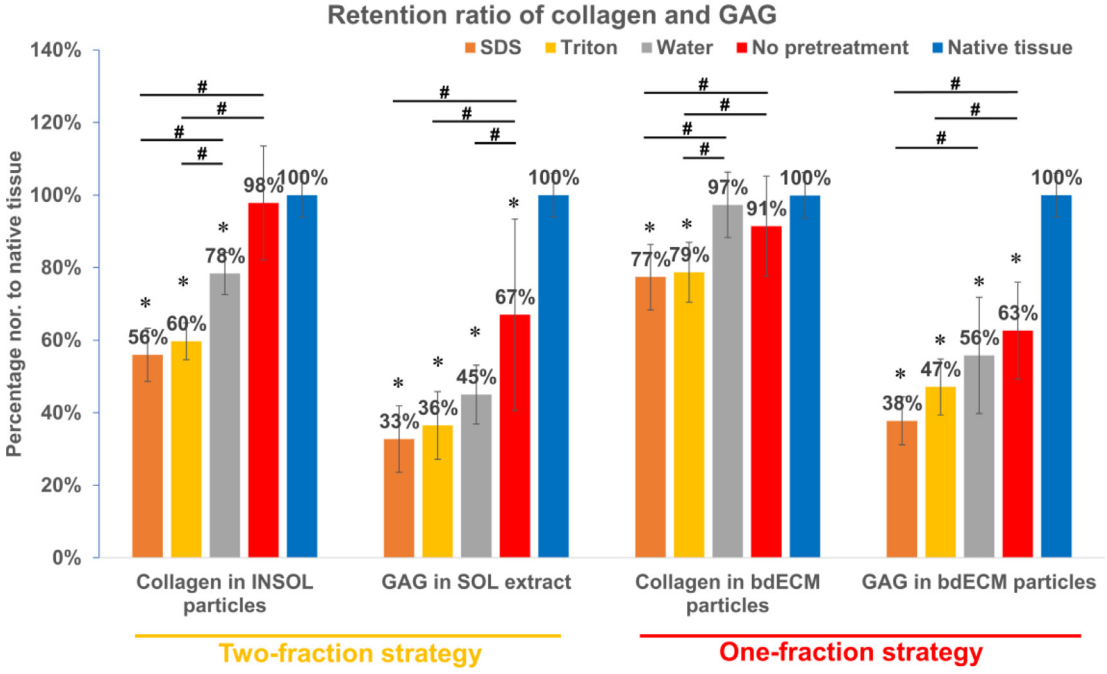

Fig. 3. Collagen and GAG retention ratio in INSOL particles and SOL extract from two-fraction decellularization strategy, and bdECM particles from one-fraction strategy with different pretreatments. Data presented as mean ± SD, $n = 9$, * $p < 0.05$ vs native tissue, # $p < 0.05$.

removal, with DNA concentration lower than the recognized decellularization criterium of 50 ng/mg [32] in both INSOL particles and SOL extract (Fig. 2). Furthermore, the percentage of harvested collagen and GAG compared with native tissue was evaluated as shown in Fig. 3. Most of the collagen and over 60% of the GAG were retained in INSOL particles and SOL extract respectively, while pretreatments, especially SDS and Triton X-100, caused a 40% collagen loss and 70% GAG loss (Fig. 3). Water pretreatment resulted in GAG loss, which is expected due to GAG affinity to water (Fig. 3). Moreover, the collagen and GAG showed higher concentrations in INSOL particles and SOL extract respectively in no pretreatment group compared to pretreatment groups, indicating higher purity after GuHCl extraction with low retention of debris and extraction reagents (Fig. 4(A)). Our method without pretreatment showed clear advantages to preserve GAG and collagen with significantly higher yield and purity compared to traditional chemical procedures since chemical and enzymatic decellularization generally lead to a significant loss of GAG and collagen [11,15,17,33]. This indicates that thorough pulverization to form small tissue particles contributes to successful detergent-free decellulariza-

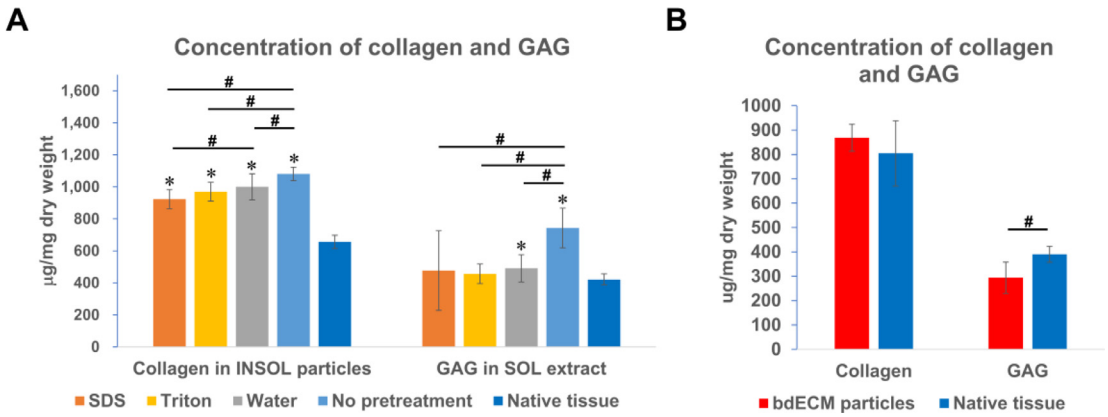

Fig. 4. Concentration of functional molecules after decellularization. (A) Collagen and GAG concentration in INSOL particles and SOL extract from two-fraction decellularization strategy with different pretreatments. (B) Collagen and GAG concentration in bdECM particles from one-fraction decellularization strategy. Data presented as mean ± SD, $n = 9$, $^{*}p < 0.05$ vs native tissue, $\#p < 0.05$.

tion with less depletion of functional components and structural integrity.

PG integrity, which was seldom reported in most previous studies [3,9,34], is crucial for the natural biological function of dECM materials. Considering the complex functional structure of PG, the inclusion of only GAG (PG subunit) in collagen biomaterials [35] does not fully restore the function of PG. Agarose gel electrophoresis in Fig. S1(A) in the Supplementary Material showed that the PG in SOL extract from the no-pretreatment group preserved the aggrecan in an intact structure, which was similar to the native tissue. This indicates good PG structure preservation in the SOL extract produced by the two-fraction strategy. Furthermore, the PG in the SOL extract from no treatment group showed a high purity, as indicated by fewer aggrecan degradation products compared to native tissue (Fig. S1(A)), which is consistent with the high GAG concentration measured in SOL extract (Fig. 4(A)). Compared to native tissue, SOL extract after SDS pretreatment contained more aggrecan monomers and its degradation products (Fig. S1(B)). Triton X-100 pretreatments did not lead to the degradation of aggrecan. However, agarose gel electrophoresis is a semi-quantitative technique, especially when different extraction methods with several steps are used; therefore, final statements about the exact amount of intact and degradation products of aggrecan should be taken cautiously. Quantitative data on PG content is given by the GAG measurement. The agarose gel electrophoresis was used for the qualitative evaluation of aggrecan and its degradation products present in the different extracts.

Our results demonstrated a successful two-fraction protease-/detergent-free decellularization method to extract functional intact cartilage components separately with high yield and purity. With the two-fraction decellularization strategy, tailored biomimetic decellularized cartilage materials can be produced using a combination of PG and collagen for cartilage tissue engineering. This offers the possibility of varying collagen:GAG composition for desired applications, and the reconstitution of ECM-based materials representative of natural cartilage.

3.2. Characterization of the cartilage dECM component produced by the one-fraction strategy

In this work we introduce a one-fraction decellularization strategy without GuHCl extraction to maintain all the functional components intact in a single dECM material (Fig. 1). DNA quantification demonstrated its successful removal (Fig. 2). Approximately 90% of the collagen and 60% of the GAG were preserved in bdECM particles, which was similar to the retained dECM components produced by the two-fraction strategy (Fig. 3). Agarose gel electrophoresis showed that aggrecan maintained an intact structure in bdECM particles generated by the one-fraction strategy (Fig. S1(C)). SDS and Triton X-100 pretreatments were also effective in DNA removal, however, they induced a significantly increased loss of GAG and collagen, similarly to the two-fraction strategy (Figs. 2 and 3). Again, SDS pretreatment resulted in an apparent increase of aggrecan monomers and its degradation products (Fig. S1(D)).

Our results demonstrate a successful one-fraction decellularization strategy to retain intact cartilage components at a high concentration in bdECM particles. Though bdECM particles showed slightly increased collagen concentration and significantly decreased GAG concentration compared to native tissue (Fig. 4(B)), GAG retention and concentration in bdECM particles generated by the novel one-fraction strategy were still 2–3 times higher than traditional decellularization methods [11]. With the improved biomimetic composition and intact molecular structure, dECM materials generated by the one-fraction strategy are promising for the restoration of the cartilage microenvironment. In addition, considering the imbalance of collagen/GAG ratio in bdECM particles after decellularization, a combination of SOL extract from the two-fraction strategy and bdECM particles from the one-fraction strategy would be an innovative and promising approach to achieve the collagen and GAG concentration in native tissue.

3.3. Histology and particle morphology

Safranin O/Fast Green and hematoxylin staining was performed to reveal the distribution of collagen (blue), PG (red), and cell nuclei (purple) simultaneously [22]. Almost all of the cell nuclei were removed in INSOL tissue and bdECM tissue compared to fresh cartilage tissue (Fig. 5(A–C)), showing the high decellularization efficiency of one/two-fraction strategies. These results confirmed the successful removal of cells and genetic material. Meanwhile, most of the PG was removed in INSOL tissue (Fig. 5(B)), which demonstrated the high PG extraction efficiency of GuHCl. The simultaneous positive staining of both collagen and PG in bdECM tissue (Fig. 5(C)), similar to the histological morphology of fresh cartilage, indicated the promising potential of bdECM particles directly made from bdECM tissue for cartilage ECM biomimicry.

Decellularized ECM in large pieces that maintained the rough architecture of the natural tissue has been directly used as a scaffold after decellularization [7,14,36]. In this study, as the cartilage tissue was pulverized for sufficient decellularization, dECM generated by the strategies introduced here could not be used as a standalone scaffold. Solubilized dECM materials are widely employed

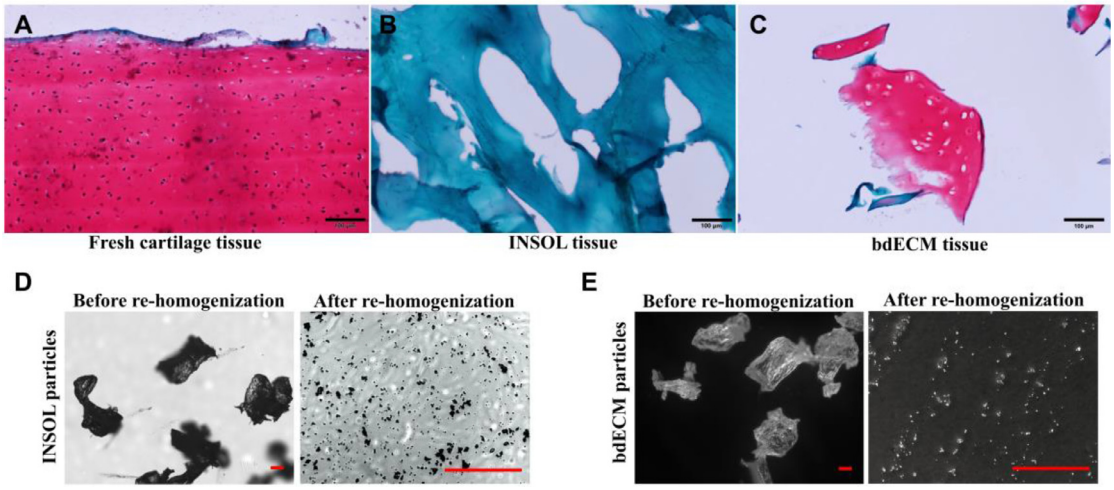

Fig. 5. Histology of decellularized cartilage tissues and morphology of cartilage particles. Safranin O/Fast Green staining on sections of (A) fresh cartilage tissue, (B) INSOL tissue, and (C) bdECM tissue. The morphology of (D) INSOL particles and (E) bdECM particles before/after re-homogenization. Scale bar: 100 μm.

to produce hydrogels or scaffolds for tissue engineering applications [11]. However, the disruption of the native microstructure or topology of the natural ECM components during solubilization digestion damages the intrinsic biological functions in solubilized dECM (e.g., dECM solubilization in acetic acid and pepsin). Alternatively, dECM can be prepared as particles, which retain the inherent tissue-specific ECM components and native ultrastructure at the particle level. In this study, decellularized particles were produced and the individual particle size was refined from hundreds of microns in diameter before re-homogenization to 4.5 ± 1.8 μm for INSOL particles (n = 100) and 5.1 ± 2.1 μm for bdECM particles (n = 100) after re-homogenization (Fig. 5(D, E)). Decellularized particles can be used to prepare composite materials, such as hydrogels [9,37,38] and bioinks [11] without a disruptive enzymatic digestion process. The uniform and small particle size contributes to their homogeneous distribution and abundantly exposed surface areas in biomaterials.

3.4. Biomimetic composite dECM-THA hydrogels as biomaterial inks

Hydrogels containing cartilage dECM have shown promising cartilage regeneration capacity due to their chondrogenic bioactivity [3,39]. However, very few studies have restored both the physiological composition and the integrity of cartilage dECM

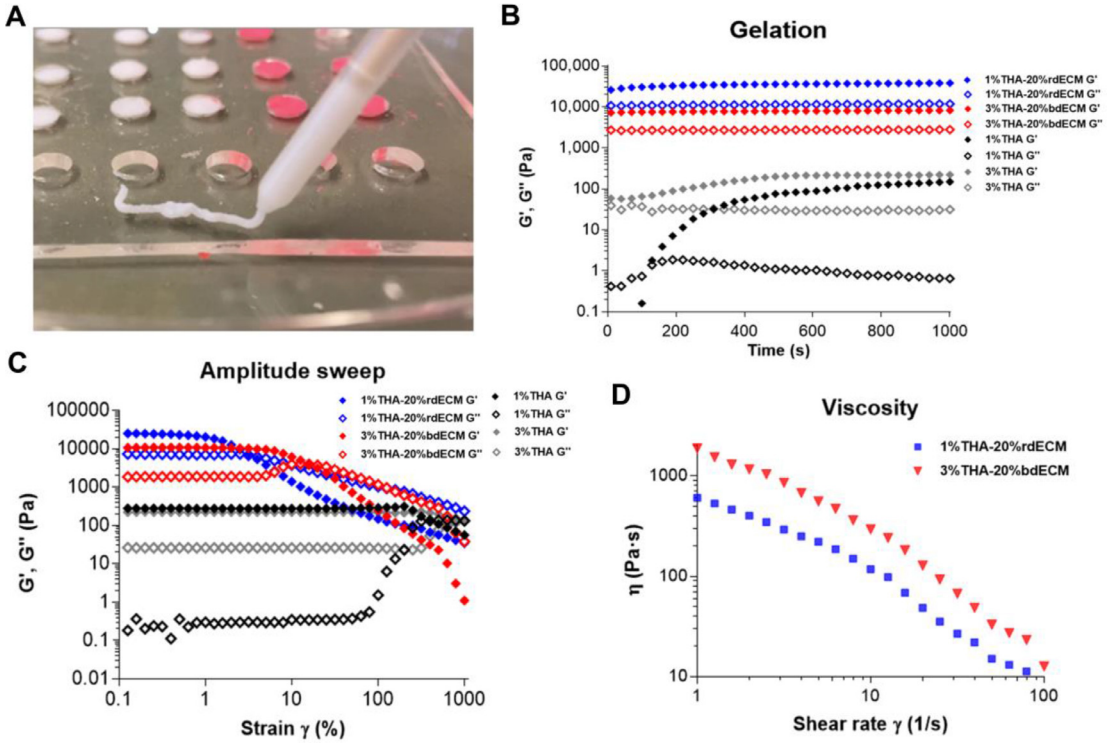

Fig. 6. Rheological characterization of the particle-embedded THA hydrogels. (A) Images showing the extrusion of particle-embedded THA composites through a positive displacement pipette to form self-supporting filaments. (B) Gelation time sweep showing shear moduli of the particle-embedded THA composites compared to THA alone. (C) Rheology tests presenting low yield and flow points in amplitude sweep and (D) decreasing viscosity with increasing shear rate in rotational test of the particle-embedded THA composites after enzymatic crosslinking. (20% rdECM: 8% SOL-12% INSOL).

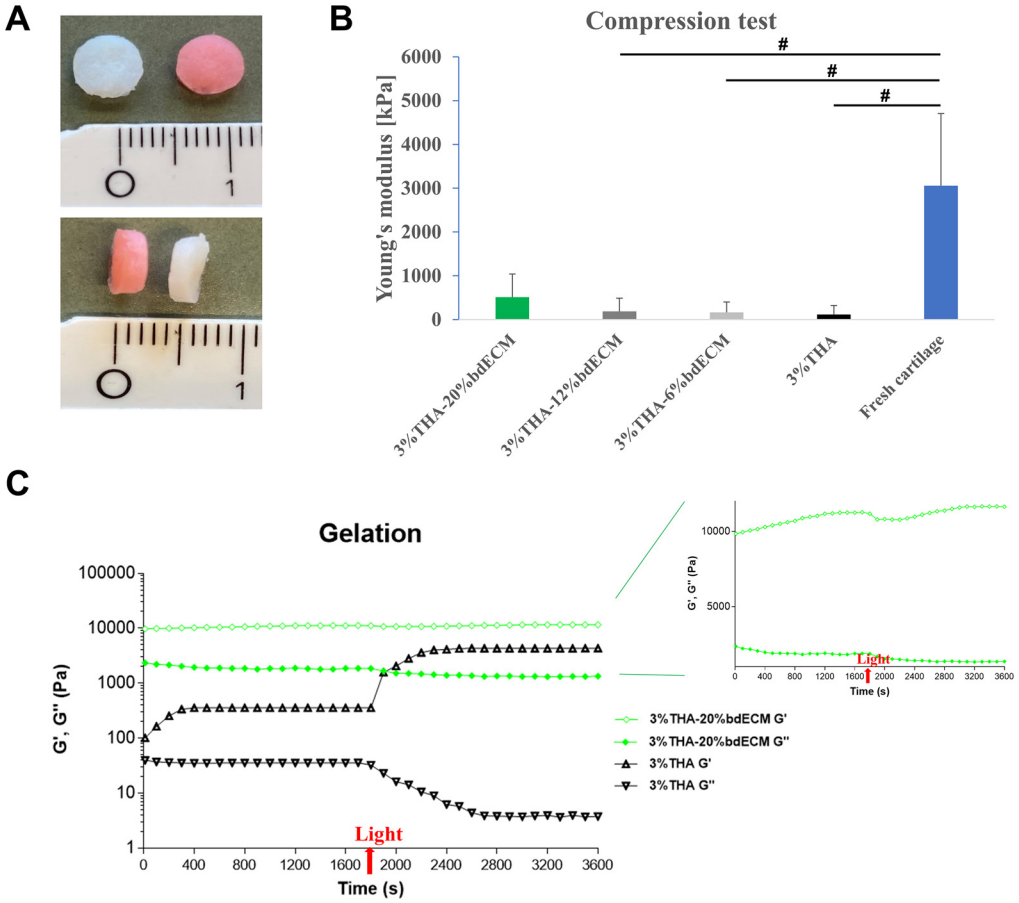

Fig. 7. Enzymatically and light crosslinked bdECM hydrogels as cartilage repair biomaterials. (A) Macroscopic images showing the hydrogel biomaterials with (red) and without (white) light crosslinking. (B) Young's moduli of different bdECM hydrogels measured in compression test. (C) Gelation test showing the storage modulus (*G'*) and loss modulus (*G''*) of 3% THA hydrogel and 3% THA-20% bdECM hydrogel during additional light crosslinking. Data presented as mean + SD, $n = 5$-9, # $p < 0.05$.

components during tissue engineering, which significantly impairs the biomimicry of the biomaterials. Water accounts for up to 80% of the cartilage ECM wet weight [1]. Collagen and PG make up the vast majority of the cartilage ECM dry weight, in which collagen accounts for 60% and PG accounts for 40% of fresh bovine articular cartilage dry weight (Fig. S2). This indicates that collagen and PG account for 12% and 8% of the total ECM wet weight respectively. In this study, intact cartilage dECM components were reconstituted at the native concentration in a hydrogel. THA hydrogels containing 20% rdECM particles (8% *w*/*w* SOL extract + 12% *w*/*w* INSOL particles) generated by the two-fraction strategy or bdECM particles (20% *w*/*w*) generated by the one-fraction strategy were prepared as biomimetic materials to approach the physiological ECM composition. As the backbone of PGs, hyaluronic acid is also a natural component of cartilage [1]. Considering the higher GAG loss compared to that of collagen during decellularization, THA as the base polymer for the hydrogel may be beneficial for rebalancing the GAG:collagen ratio. To ensure the stability of biomimetic hydrogels, 3% THA was firstly tested for sufficient crosslinking [24]. However, 8% SOL extract could not be completely dissolved in 3% THA solution (Fig. S3). Thus, the bdECM particles were embedded in 3% THA, while the rdECM particles were embedded in 1% THA to successfully form the biomimetic hydrogel.

Mild enzymatic crosslinking was applied to generate particle-embedded THA hydrogel precursors as bioinks. Upon manual extrusion, the biomaterial inks formed self-supporting filaments (Fig. 6(A)). Both rdECM and bdECM particles significantly increased the shear moduli of the THA hydrogels (Fig. 6(B)), which resulted in improved mechanical properties of biomaterial inks. The low yield and flow points of these biomaterial inks (Fig. 6(C)) enabled extrusion at low pressures to reduce the shear stress, which is critical to preserve cell viability during printing. THA's shear-thinning, indicative of good printability [40], was preserved in both composites (Fig. 6(D)). To further improve the mechanical properties of the printed hydrogel constructs, 1% THA-20% rdECM may be combined with other rheological enhancers [11]. Overall, these results indicate the potential of rdECM and bdECM particle-embedded THA hydrogels as biomaterial inks for 3D printing.

3.5. Biomimetic dECM-THA hydrogels as cartilage repair biomaterials

Particle-embedded THA hydrogels can be fabricated directly as biomaterials for cartilage tissue engineering. Additionally, a second crosslinking was necessary to enhance the structural stability of the enzymatically crosslinked, but still soft hydrogel (Fig. 7(A)). We screened the properties of THA hydrogels containing different concentrations of rdECM particles (12% INSOL particle + 4%/2%/1% SOL extract) or bdECM particles (20%, 12%, 6%) for their ability to form a biomimetic hydrogel. The rdECM particles interfered with the eosin Y-based light crosslinking, resulting in decreased storage moduli (G') of rdECM particle-embedded hydrogels (Fig. S4). THA hydrogels containing rdECM particles also showed a high swelling ratio (Fig. S5) and massive loss and low retention of GAG and collagen (Figs. S6 and S7), indicating the instability of these hydrogels for long-term incubation in DMEM at 37 °C. Hence, the rdECM particle-embedded THA hydrogels do not possess long-term stability as self-standing biomaterials. On the other side, compression moduli of THA hydrogels containing 12% and 6% bdECM particles

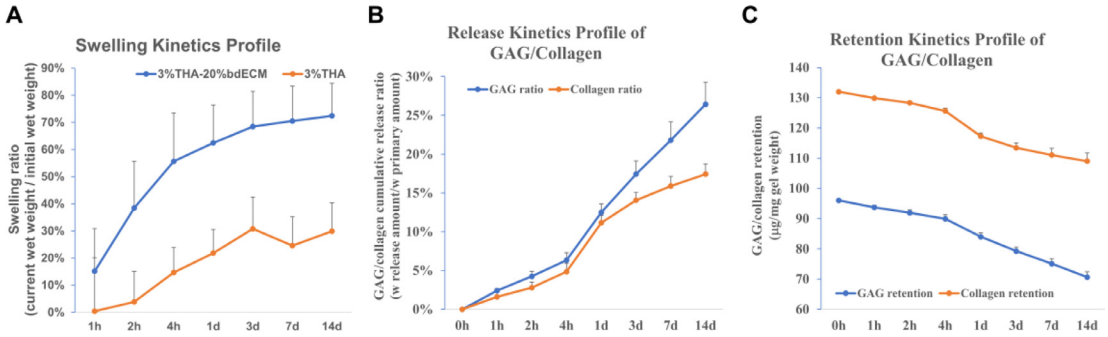

Fig. 8. Characterization of 3% THA-20% bdECM hydrogels. (A) Swelling property of the hydrogels. (B) Release kinetics profile of GAG and collagen during long-term incubation. (C) Retention kinetics profile of GAG and collagen during long-term incubation. Data presented as mean + SD, $n = 6$.

were significantly lower than native cartilage tissue, whereas the compressive Young's modulus of 3% THA-20% bdECM hydrogel was approaching the values measured for fresh bovine cartilage (Fig. 7(B)). Thus, the biomimetic 3% THA-20% bdECM hydrogel was used for further rheology and stability tests. Compared to 3% THA hydrogel, the shear modulus of enzymatically and light crosslinked 3% THA-20% bdECM hydrogel was significantly increased. During the gelation process of 3% THA-20% bdECM hydrogel, the storage modulus (G') slightly decreased after the light crosslinking was applied, and then showed an increase until the end of the test (Fig. 7(C)). This indicates that bdECM particles strongly contribute to the rheological properties of the composites, which brings a much smaller variation of rheological properties upon exposure to light. The biomimetic hydrogel showed a swelling ratio of ~70% (Fig. 8(A)) and lost 26.4% of the GAG and 17.4% of the collagen (Fig. 8(B)) after 2 weeks of incubation in DMEM at 37 °C, indicating the long-term stability of the hydrogel. The hydrogel retained 70.6 ± 2.7 μg/mg gel weight of GAG and 109.0 ± 1.7 μg/mg gel weight of collagen after 2 weeks of in vitro incubation (Fig. 8(C)), very similar to the physiological composition of cartilage ECM [1]. The bdECM particles maintain the intact PG structure, the innate collagen-PG interaction, and the natural composition of cartilage ECM. The biomimetic bdECM hydrogels possess superior long-term stability with an enhanced mechanical property level. These results indicate that bdECM hydrogels have a stronger potential as biomimetic cartilage biomaterial compared to rdECM hydrogels. Our previous studies have shown good cytocompatibility of the THA enzymatic and light crosslinking [24–27]. Further investigations are needed to determine the biological properties of THA-dECM hydrogels.

4. Conclusion

In the current study, we established one/two-fraction decellularization strategies to produce decellularized cartilage components with an intact molecular structure, high yield, and without the disruptive processes of enzymatic digestion and detergent treatments. The resulting dECM materials provide a biomimetic microenvironment close to native tissue for cartilage regeneration. With these new strategies, the natural composition of cartilage ECM can be restored in rdECM particles through a tailored combination of PG and collagen produced by the two-fraction strategy and bdECM particles produced by the one-fraction strategy. Soft enzymatically crosslinked rdECM or bdECM particle-based THA composite hydrogels demonstrated rheological properties suitable for 3D printing with increased shear moduli, low yield and flow points, and shear-thinning properties. Light crosslinked bdECM particle-based hydrogels achieved long-term stability, and close-to-natural composition during long-term incubation. In conclusion, biomimetic hydrogels containing cartilage dECM particles with an intact molecular structure and a natural composition are promising biomaterials for cartilage repair.

Declaration of Competing Interest

The authors declare that they have no known competing financial interests or personal relationships that could have appeared to influence the work reported in this paper.

Acknowledgments

This study was funded by AO Foundation and AOSpine International. Peng Guo and Nan Jiang were funded by Sino Swiss Science and Technology Cooperation Program (Nos. EG-CN_01–032019 and EG-CN_04–042018) and China Scholarship Council. MD and GM gratefully acknowledge funding from the Swiss National Science Foundation (SNSF, No. 310030E_189310).

Supplementary materials

Supplementary material associated with this article can be found, in the online version, at doi:10.1016/j.jmst.2023.03.019.

References

[1] A.J. Sophia Fox, A. Bedi, S.A. Rodeo, Sports Health 1 (6) (2009) 461–468.
[2] C. Vinatier, J. Guicheux, Ann. Phys. Rehabil. Med. 59 (3) (2016) 139–144.
[3] Y.S. Kim, M. Majid, A.J. Melchiorri, A.G. Mikos, Bioeng. Transl. Med. 4 (1) (2019) 83–95.
[4] A.J. Vernengo, S. Grad, D. Eglin, M. Alini, Z.J.A.F.M. Li, Adv. Funct. Mater. 30 (44) (2020) 1909044.
[5] W. Shen, K. Berning, S.W. Tang, Y.W. Lam, Tissue Eng. Part C-Methods 26 (4) (2020) 201–206.
[6] F. Forouzesh, M. Rabbani, S. Bonakdar, J, Med. Signals Sens. 9 (4) (2019) 227–233.
[7] C. Xia, S. Mei, C. Gu, L. Zheng, C. Fang, Y. Shi, K. Wu, T. Lu, Y. Jin, X. Lin, P. Chen, Mater. Sci. Eng. C Mater. Biol. Appl. 101 (2019) 588–595.
[8] M. Nouri Barkestani, S. Naserian, G. Uzan, S. Shamdani, J. Tissue Eng. 12 (2021) 2041731420983562.
[9] T. Novak, B. Seelbinder, C.M. Twitchell, S.L.P. Voytik-Harbin, C.P.P. Neu, Adv. Funct. Mater. 26 (30) (2016) 5427–5436.
[10] L. Zhou, P. Guo, M. D'Este, W. Tong, J. Xu, H. Yao, M.J. Stoddart, G.J.V.M. van Osch, K.K. Ho, Z. Li, L. Qin, Engineering 13 (2022) 71–90.
[11] F. Pati, J. Jang, D.H. Ha, S. Won Kim, J.W. Rhie, J.H. Shim, D.H. Kim, D.W. Cho, Nat. Commun. 5 (2014) 3935.
[12] L. Sun, H. Hou, B. Li, Y. Zhang, Int. J. Biol. Macromol. 99 (2017) 8–14.
[13] V. Beachley, G. Ma, C. Papadimitriou, M. Gibson, M. Corvelli, J. Elisseeff, J. Biomed. Mater. Res. A 106 (1) (2018) 147–159.
[14] Y. Chen, J. Chen, Z. Zhang, K. Lou, Q. Zhang, S. Wang, J. Ni, W. Liu, S. Fan, X. Lin, Cell Tissue Res. 370 (1) (2017) 41–52.
[15] T. Ghassemi, N. Saghatoleslami, N. Mahdavi-Shahri, M.M. Matin, R. Gheshlaghi, A. Moradi, J. Tissue Eng. Regen. Med. 13 (10) (2019) 1861–1871.
[16] H. Yin, Y. Wang, Z. Sun, X. Sun, Y. Xu, P. Li, H. Meng, X. Yu, B. Xiao, T. Fan, Y. Wang, W. Xu, A. Wang, Q. Guo, J. Peng, S. Lu, Acta Biomater. 39 (2016) 96–109.
[17] Z. Luo, Y. Bian, W. Su, L. Shi, S. Li, Y. Song, G. Zheng, A. Xie, J. Xue, Am. J. Transl. Res. 11 (3) (2019) 1417–1427.
[18] S.W. Sajdera, V.C. Hascall, J. Biol. Chem. 244 (1) (1969) 77–87.

[19] J. Antoniou, T. Steffen, F. Nelson, N. Winterbottom, A.P. Hollander, R.A. Poole, M. Aebi, M. Alini, J. Clin. Invest. 98 (4) (1996) 996–1003.
[20] D. Heinegard, Y. Sommarin, E. Hedbom, J. Wieslander, B. Larsson, Anal. Biochem. 151 (1) (1985) 41–48.
[21] J. Antoniou, F. Mwale, C.N. Demers, G. Beaudoin, T. Goswami, M. Aebi, M. Alini, Spine 31 (14) (2006) 1547–1554.
[22] K. Li, P. Zhang, Y. Zhu, M. Alini, S. Grad, Z. Li, Front. Bioeng. Biotechnol. 9 (2021) 787020.
[23] C. Loebel, M. D'Este, M. Alini, M. Zenobi-Wong, D. Eglin, Carbohydr. Polym. 115 (2015) 325–333.
[24] A. Schwab, C. Helary, R.G. Richards, M. Alini, D. Eglin, M. D'Este, Mater. Today Bio. 7 (2020) 100058.
[25] F. Staubli, M.J. Stoddart, M. D'Este, A. Schwab, Acta Biomater. 143 (2022) 253–265.
[26] R. Ziadlou, S. Rotman, A. Teuschl, E. Salzer, A. Barbero, I. Martin, M. Alini, D. Eglin, S. Grad, Mater. Sci. Eng. C-Mater. Biol. Appl. 120 (2021) 111701.
[27] B. Derkus, B.O. Okesola, D.W. Barrett, M. D'Este, T.T. Chowdhury, D. Eglin, A. Mata, Acta Biomater. 109 (2020) 82–94.
[28] R.L. Davies, N.J. Kuiper, Bioengineering 6 (1) (2019) 22 Basel.
[29] P.N. Nonaka, N. Campillo, J.J. Uriarte, E. Garreta, E. Melo, L.V. de Oliveira, D. Navajas, R. Farre, J. Biomed. Mater. Res. A 102 (2) (2014) 413–419.
[30] J. Fernandez-Perez, M. Ahearne, Sci. Rep. 9 (1) (2019) 14933.
[31] H. Lu, T. Hoshiba, N. Kawazoe, G. Chen, J. Biomed. Mater. Res. A 100 (9) (2012) 2507–2516.
[32] P.M. Crapo, T.W. Gilbert, S.F. Badylak, Biomaterials 32 (12) (2011) 3233–3243.
[33] D.M. Giraldo-Gomez, B. Leon-Mancilla, M.L. Del Prado-Audelo, A. Sotres-Vega, J. Villalba-Caloca, D. Garciadiego-Cazares, M.C. Pina-Barba, Mater. Sci. Eng. C–Mater. Biol. Appl. 59 (2016) 930–937.
[34] T.K. Sampath, A.H. Reddi, Proc. Natl. Acad. Sci. U. S. A. 78 (12) (1981) 7599–7603.
[35] X. Jiang, J. Liu, Q. Liu, Z. Lu, L. Zheng, J. Zhao, X. Zhang, Biomater. Sci. 6 (6) (2018) 1616–1626.
[36] P. Das, Y.P. Singh, B.B. Mandal, S.K. Nandi, Methods Cell Biol. 157 (2020) 185–221.
[37] Y. Lu, Y. Wang, H. Zhang, Z. Tang, X. Cui, X. Li, J. Liang, Q. Wang, Y. Fan, X. Zhang, ACS Appl. Mater. Interfaces 13 (21) (2021) 24553–24564.
[38] J. Visser, D. Gawlitta, K.E. Benders, S.M. Toma, B. Pouran, P.R. van Weeren, W.J. Dhert, J. Malda, Biomaterials 37 (2015) 174–182.
[39] S. Bordbar, N. Lotfi Bakhshaiesh, M. Khanmohammadi, F.A. Sayahpour, M. Alini, M. Baghaban Eslaminejad, J. Biomed. Mater. Res. A 108 (4) (2020) 938–946.
[40] C. Loebel, C.B. Rodell, M.H. Chen, J.A. Burdick, Nat. Protoc. 12 (8) (2017) 1521–1541.